EKSPLOATACJA I NIEZAWODNOŚĆ MAINTENANCE AND RELIABILITY

Eksploatacja i Niezawodnosc – Maintenance and Reliability

Volume 24 (2022), Issue 4

journal homepage: http://www.ein.org.pl

Article citation info:
Sliwinski P. The influence of pressure drop on the working volume of a hydraulic motor. Eksploatacja i Niezawodnosc – Maintenance and Reliability 2022; 24 (4): 747–757, http://doi.org/10.17531/ein.2022.4.15

The influence of pressure drop on the working volume of a hydraulic motor

Indexed by: Web of Science Group

Pawel Sliwinski [a]

[a] Gdansk University of Technology, Faculty of Mechanical Engineering and Ship Technology, u. Narutowicza 11/12, 80-233 Gdansk, Poland

Highlights

- New method of determination ot the working volume of a hydraulic motor has been proposed.
- The actual working volume is a function of the pressure drop in motor working chambers.
- The actual working volume is bigger than the theoretical working volume.
- The actual working volume should be taken to evaluate losses in a hydraulic motor.

Abstract

Reliability and maintenance analysis of hydraulic positive machines basicly focused on the processes of their wear and failure. But in order to correctly assess the mechanical and volumetric efficiency of a hydraulic motor, both at the stage of development research or at the stage of control tests during its exploitation, the working volume of this motor must be correctly determined. Therefore this paper proposes a new method of assessment of the size of the working volume of a hydraulic motor. It has been shown that the hydraulic motor absorbency per one revolution of this motor shaft is a non-linear function of pressure drop in working mechanism of the motor and non-linear function of motor rotational speed. Thus the relation between the working volume of a hydraulic motor and the pressure drop in the motor working mechanism is a non-linear function. This working volume as a funcition of pressure drop has been called the actual working volume. The correctness of the proposed method was confirmed experimentally.

Keywords

theoretical working volume, actual working volume, hydraulic motor, satellite motor, volumetric efficiency, mechanical efficiency.

1. Introduction

Reliability and maintenance analysis of hydraulic drives is mainly oriented to hydraulic positive displacement machines (pump, motor, cylinder) [4, 5, 8, 17, 26, 27, 42]. This machines are the core of modern hydraulic system [1, 9, 13, 14, 19, 29]. In overall performance of the hydraulic system the behavior of hydraulic motor has an important meaning [11, 12]. The basic characteristics of the hydraulic motor and pump, such as characteristics of volumetric losses, mechanical losses and pressure losses are important to assess its volumetric efficiency and mechanical-pressure efficiency [28, 31, 53, 54]. Thus it is important for designers of a hydraulic system [52]. The knowledge of the above mentioned characteristics is also very important from the point of view of exploitation not only of the hydraulic motor itself, but also the entire hydraulic system [16, 46]. So far, the correct assessment of the losses in hydraulic motor, and thus partial efficiencies, depends on theoretical working volume q_t. The value of theoretical working volume q_t is taken constant in the whole range of the pressure drop Δp in the motor. Furthermore the theoretical working volume q_t is independent on the motor speed n [2, 3]. Thus, improper adoption of the theoretical working volume q_t may, during the exploitation of the hydraulic system at different pressure drop in the motor inflow port, results in a different than required shaft rotational speed n than expected [39, 40, 41].

So far, in industrial practice, but also in laboratories, the theoretical working volume q_t is determined in a very simplified way. The liquid compressibility is omitted. Similarly, the pressure drop Δp_{ich} in the internal channels of the motor is also treated as insignificant and is negligible. It means that the pressure drop Δp in a motor is the same as the pressure drop Δp_i in the working chambers of this motor [2]. This is, of course, a considerable simplification.

The theoretical working volume q_t is not the same as the so-called geometric working volume q_g. The geometric working volume q_g results from the geometrical dimensions of the working chambers and is determined by constructors of a hydraulic motor, pump or other positive displacement devices like a rotational hydraulic dumper [43, 56, 57]. The formulas describing the geometric working volume q_g are not the same for all types of positive displacement machines and very often these formulas are derived with some simplifications. In this way, the simplifications result in error of up to 3% for gear pumps [3, 43]. Furthermore, in the real (manufactured) motor, the geometric

E-mail addresses: P. Sliwinski (ORCID: 0000-0003-1332-3661): pawel.sliwinski@pg.edu.pl

volume q_g differs from that determined based on the design documentation. The cause are loosenesses between working mechanism elements, machining errors, assembly errors, etc [2, 3].

As a result of the motor load by torque M in the motor working chambers is generated pressure differential Δpi. This causes elastic deformation of the engine working chambers. Thus, the working volume of the loaded motor is bigger than motor without load [36, 37]. Similar phenomena observed Osiecki in a prototype of axial piston pump [25]. In this way the working volume depends on the pressure drop Δp_i in the working chambers of the motor and was called the actual working volume q_r [36, 37].

If $\Delta p_i = 0$ then $q_r = q_t$, where q_t is the theoretical working volume [36, 37]. Therefore, both the geometric volume q_g and the theoretical working volume q_t are different from the actual working volume q_r. Booth q_t and q_g are should not be used to determine losses in motor and thus to calculate partial efficiencies of this motor [36, 37].

The first works on the methodology of determining the theoretical working volume appeared in the 1940s and 1960s. These were the work of Wilson (1949) [51], Schlosser and Hilbrands (1963) [32, 33]. Then the works of Toet and Balawender in 1970s and again in 2019 [2, 3, 44, 45]. The Toeth method was also described by Post in [30]. The methodology proposed by Toet and Balawender is based on characteristics of the flow rate Q to motor in the function the rotational speed n at constant pressure drops Δp in the motor. In work [36] Sliwinski presented a new look on the Balawender method. Moreover, in [37] Sliwinski proposed another new method for determining the working volume. In Sliwinski's method the characteristics of effective absorbency of the motor were used.

The adoption of the theoretical working volume q_t for assessment of the losses in displacement machines introduces a significant error [36, 37]. Furthermore in [36, 37] has been demonstrated that:

– the liquid compressibility has the influence on the theoretical working volume q_t and the actual working volume q_r;
– to assess volumetric and mechanical losses in a hydraulic motor should be use the actual working volume q_r.

The simplest method of assessment the theoretical working volume has been shown in the ISO standard [7, 10]. But this method gives an inaccurate result and in scientific considerations it is rather not used. According to Kim, the theoretical working volume can be determined by analysis a flow rate only in a single chamber of the working mechanism [15]. Similar method is proposed by Manring and Williamson [21]. These methods have no practical application in real tests of hydraulic motors and also pumps. The other method, called Latin Hyperspace Sampling (LHS), is proposed by Michael and Garcia-Bravo [22].

Balawender proved that based on the characteristics of the hydraulic motor absorbency q_e per one revolution of the motor shaft vs pressure drop Δp in this motor at n=const is posible to determine the theoretical working volume q_t [2, 3]. This method will be briefly presented later in this article. Based on Balawender method, the proposed new method of determination the actual working volume q_r and the theoretical working volume q_t of a hydraulic motor is described in this article. The correctness of this method was experimentally verified.

Hydraulic motors with a satellite mechanism are the object of interest of many researchers and set a new trend in research in the field of hydraulic positive displacement machines. This is evidenced by the works [47, 48, 49, 50, 56]. These motors are also the main object of the author's scientific interests. Therefore a satellite hydraulic motor was selected for the experimental test. Its construction is presented in Section 5.1.

2. Flow rate in hydraulic motor

The basis for determining the theoretical working volume q_t and the actual working volume q_r of a hydraulic motor is the precise measurement of the flow rate into or out of the motor and the measurement of external leakage (if any). Generally, is recommended to use two flow meters – in the inflow line and in the outflow line of the tested motor (Fig. 1) [2,3]. But Toeth used only one flow meter installed in the motor inlet line [44, 45].

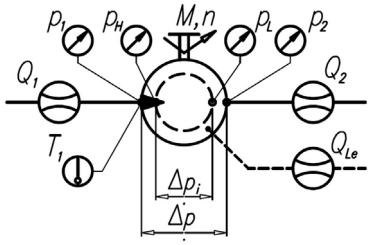

Fig. 1. Parameters measured in a hydraulic motor [37]: Q_1 – flow rate to the motor, Q_2 – flow rate from the motor, Q_{Le} – external leakage; p_1 – pressure in the inflow port, p_2 – pressure in the outflow port, p_H – pressure in the high-pressure working chamber, p_L – pressure in the low-pressure working chamber, M – torque, n – rotational speed, T_1 – liquid temperature in inflow port, Δp – pressure drop in the motor, Δp_i – pressure drop in the motor working chambers.

To correctly determine the theoretical and actual working volume, it is necessary to analyze the flow balance in the hydraulic motor. The general model of the flow rate in a hydraulic motor is proposed by Balawender and is described by [2, 3]:

$$Q_1 = \underbrace{Q_g + Q_u + Q_k + Q_C + Q_{Li}}_{Q_2} + Q_{Le} \tag{1}$$

where [2, 3]:

Q_g – the flow rate dependent on the geometric working volume q_g and rotational speed n,
Q_u – the flow rate lifted in the gaps,
Q_k – the flow rate dependent on the working chambers cyclic elastic deformation,
Q_C – the flow rate caused by liquid compressibility,
Q_{Li} – the flow rate from high-pressure working chambers to low-pressure working chambers (internal leakage),
Q_{Le} – the external leakage.

Another model is proposed by Sliwinski. This model is described by general formula [37, 39, 40]:

$$Q_1 = \underbrace{Q_t + \Delta Q_L + Q_{Lfg} + Q_{CU}}_{Q_L} + Q_{Le} \tag{2}$$

where:

Q_t – the theoretical flow rate in the motor:

$$Q_t = q_t \cdot n \tag{3}$$

ΔQ_L – the component of volumetric losses depends on liquid compressibility and rotational speed of the motor [39, 40]:

$$\Delta Q_L = \underbrace{\left(C_q \cdot \Delta p_i + \frac{C_{id}}{n^{0,5}} \right) \cdot m^2 \cdot H \cdot n}_{\Delta q_L} \tag{4}$$

m – the teeth module in the satellite mechanism,
H – the height of the satellite mechanism,
C_q, C_{id} – coefficients,
Δp_i – the pressure drop in working mechanism of the motor, defined as [35, 38]:

$$\Delta p_i = \Delta p - \Delta p_{ich} \tag{5}$$

Δp_{ich} – the pressure drop in the motor internal channels [35, 38]:

$$\Delta p_{ich} = C_t \cdot \rho \cdot Q_2^2 + C_l \cdot \nu \cdot \rho \cdot Q_2 \tag{6}$$

C_l, C_t – the constant of the laminar and turbulent flow component respectively,
ν – the kinematic viscosity,
ρ – the density of liquid,
Q_{Lfg} – the flow rate in flat clearances of working mechanism,
Q_{CU} – the flow rate in commutation unit clearances.

The external leakage Q_{Le} has been defined as [37, 39, 40]:

$$Q_{Le} = Q_{Le1} + Q_{Le2} \tag{7}$$

Q_{Le1} – the leakage from the high-pressure working chambers (with the pressure p_H) to the outside of the motor (with the pressure equal zero),
Q_{Le2} – the leakage from the low-pressure working chambers (with the pressure p_L) to the outside of the motor (with the pressure equal zero).

The methodology of determination of Δp_i and Δp_{ich} is widely described in the works [35, 36, 38, 39]. Similarly, each component of the above mathematical model has been described in detail in publications [35, 38, 39] and will not be discussed in more detail here.

3. Balawender's method of determining the theoretical working volume

The method of determining the theoretical working volume based on characteristic $q_e = f(\Delta p)_{n=const.}$ was developed by Balawender in 1974 [3]. q_e is called the effective absorbency of the motor per one revolution of its shaft and is defined as:

$$q_{e1} = \frac{Q_1}{n} \tag{8}$$

$$q_{e2} = \frac{Q_2}{n} \tag{9}$$

that is:

$$q_{e1} = \underbrace{q_g + q_u + q_k + q_{C1}}_{q_{w1}} + \underbrace{\frac{Q_{Le1}}{n}}_{q_{L1}} \tag{10}$$

$$q_{e2} = \underbrace{q_g + q_u + q_k + q_{C2}}_{q_{w2}} + \underbrace{\frac{Q_{Le2}}{n}}_{q_{L2}} \tag{11}$$

where $q_g = Q_g/n$, $q_u = Q_u/n$ etc.

If the Δp_i decreases to zero then for a given constant motor speed n [3]:

$$\lim_{\Delta p_i \to 0} (q_{e1})_{(n)} = q_{t1(n)} + \frac{1}{n} \cdot \lim_{\Delta p_i \to 0} Q_{Le1} \tag{12}$$

$$\lim_{\Delta p_i \to 0} (q_{e2})_{(n)} = q_{t2(n)} - \frac{1}{n} \cdot \lim_{\Delta p_i \to 0} Q_{Le2} \tag{13}$$

and:

$$\lim_{\Delta p_i \to 0} Q_{Le1} = \lim_{\Delta p_i \to 0} Q_{Le2} = \frac{1}{2} \cdot \lim_{\Delta p_i \to 0} Q_{Le} = 0 \tag{14}$$

Then from the equations (12) and (13) is:

$$q_{t1(n)} = \lim_{\Delta p_i \to 0} (q_{e1})_{(n)} - \frac{1}{2 \cdot n} \cdot \lim_{\Delta p_i \to 0} Q_{Le} \tag{15}$$

$$q_{t2(n)} = \lim_{\Delta p_i \to 0} (q_{e2})_{(n)} + \frac{1}{2 \cdot n} \cdot \lim_{\Delta p_i \to 0} Q_{Le} \tag{16}$$

But the theoretical forking volume for a given constant motor speed n is:

$$q_{t(n)} = \frac{1}{2} \cdot \left(q_{t1(n)} + q_{t2(n)} \right) \tag{17}$$

According to Balawender the test of motor can be carried out at limited amount of speed n, for example at minimum speed, nominal speed and maximum speed. Then the final theoretical working volume q_t shoult be taken as:

$$q_t = \frac{1}{z} \cdot \left(q_{t(n)1} + q_{t(n)2} + \ldots + q_{t(n)z} \right) \tag{18}$$

Furthermore, Balawender claims that his metod gives a satisfactory result of q_t only at one motor speed n. Then $q_t = q_{t(n)}$.

The graphical implementation of Balawender's method is shown in Fig. 2

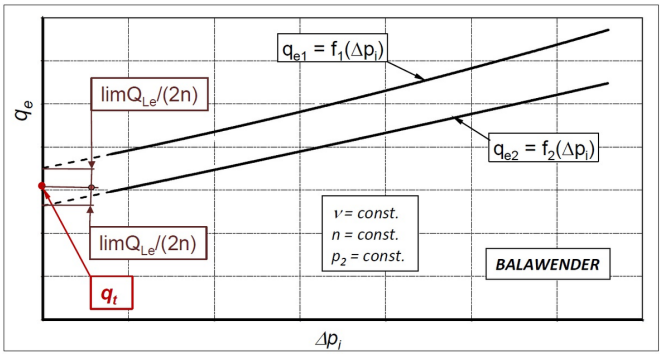

Fig. 2. The graphical implementation of Balawender's method [3]

Balawender recommends that [2, 3]:

a) the characteristics $q_e = f(\Delta p_i)$ obtained from the experimental data (Fig. 2) should be described by the formula:

$$q_{e1} = q_{e1(\Delta pi=0)} \pm \frac{a_1}{n} \cdot (\Delta p_i)^{b_1} \tag{19}$$

$$q_{e2} = q_{e2(\Delta pi=0)} \pm \frac{a_2}{n} \cdot (\Delta p_i)^{b_2} \tag{20}$$

b) the characteristic of external leakage Q_{Le} should be described by the formula:

$$Q_{Le} = Q_{Le(\Delta pi=0)} + a_Q \cdot (\Delta p_i)^{b_Q} \tag{21}$$

where the values of the constants a_1, a_2, a_Q, b_1, b_2 and b_Q should be determined by the least squares method.

4. Proposed new method of determining the actual and theoretical working volume

The bigges disadvantage of the Balawender method is the assumption of the theoretical working volume q_t as the average of the working volumens calculated for various constant rotational speeds. In addition, Balawender argues, that the theoretical working volume q_t can be determined even with the one constant rotational speed n [2, 3]. Thus, Balawender does not specify the effect of the motor speed n on the theoretical working volume q_t. Sliwinski showed that the volumetric losses in the hydraulic motor are nonlinear function of speed n (see formulas (2) and (4)).

Another disadvantage of the Balawender method is, recommended by him, the method of describing the effective absorbency q_e (equations (19) and (20)). These formulas will only describe the absorbency well if the leakage in the motor will increase non-linearly. A non-linear increase in leakage occurs when, as a result of pressure increase, there is an increase in the clearances in the working mechanism. Such a phenomenon occurs in motor that is not equipped with a clearance compensation unit in the working mechanism [40].

4.1. Influence of pressure on the working volume

Balawender and Toeth adopted the simplification that the increase in working volume of a motor is a linear function of pressure drop in the motor [2, 3, 44, 45]. In fact, each dimension of the engine working chamber changes linearly under the pressure. Sliwinski in [36] showed that the working volume changes nonlinearly in the function of the pressure drop Δp_i. Therefore, in loaded motor the theoretical working wolume q_t is not equal the actual working wolume q_r. The actual working volume q_r is described by the following formula [36, 37]:

$$q_r = q_t + \underbrace{\left(C_{q1} \cdot \Delta p_i + C_{q2} \cdot \Delta p_i^{\,2} + C_{q3} \cdot \Delta p_i^{\,3}\right) m^2 \cdot H}_{\Delta q_p} \tag{22}$$

where Δq_p is the change in working volume of the loaded motor. So, the increase in working volume Δq_p can not be the reason of the mechanical and volumetric losses in the motor. Therefore the relationship (4) should take the form:

$$\Delta Q_L = \underbrace{\left(\frac{C_{id}}{n^{0.5}}\right) \cdot m^2 \cdot H}_{\Delta_{qL}} \cdot n \tag{23}$$

where Δq_L is the change in unit volumetric losses (that is volumetric losses per one revolution of the motor shaft). It can be assumed that the influence of pressure drop Δp_i in motor working mechanism on the Δq_L is very small and for father consideration can be neglected. The ΔQ_L is mainly caused by the movement of liquid in the spaces between the mating teeth during rotation of the working mechanism with speed n [39, 40].

4.2. Flow rate in a hydraulic motor

Taking into account the formula (22) the flow rate in a motor can be written with the following equation:

$$Q_1 = \underbrace{q_r}_{Q_r} \cdot n + \underbrace{\Delta q_L \cdot n + Q_C + Q_{Lfg} + Q_{CU} + Q_{Le}}_{Q_L} = Q_2 + Q_{Le} \tag{24}$$

Immediately from the measured datas the flow rate per one revolution of the motor shaft q_e should be calculated according to formulas (8) and (9):

$$q_{e1} = q_r + \cdot q_L + \frac{Q_C + Q_{Lfg} + Q_{CU} + Q_{Le}}{n} \tag{25}$$

$$q_{e2} = q_r + \cdot q_L + \frac{Q_C + Q_{Lfg} + Q_{CU}}{n} \tag{26}$$

where:

- Q_C – the flow rate component depends on the liquid compressibility and can be described as a sum:

$$Q_C = Q_{C1} + Q_{C2} \tag{27}$$

- Q_{C1} – the flow rate component depends on the pressure difference $p_1 - p_H$ ($p_1 > p_H$) and describes as [36, 37]:

$$Q_{C1} = Q_1 \cdot \int_{p_H}^{p_1} \frac{1}{K_{Z(p)}} dp \tag{28}$$

- Q_{C2} – the flow rate component depends on the pressure difference $p_H - p_2$ ($p_H >> p_2$) and describes as [36, 37]:

$$Q_{C2} = Q_2 \cdot \int_{p_2}^{p_H} \frac{1}{K_{Z(p)}} dp \tag{29}$$

- $K_{Z(p)}$ – the tangential isentropic bulk modulus (Fig. 7) [36, 54, 55].

Because the pressure drop Δp_i in the working mechanism influences on the volumetric losses Q_L then the Q_1 and Q_2 should be related to pressure p_H in high pressure working chambers. Then:

$$Q_{1(p_H)} = Q_1 + Q_{C1} \tag{30}$$

$$Q_{2(p_H)} = Q_2 - Q_{C2} \tag{31}$$

The flow rate $q_{e(pH)}$ related to the pressure p_H should be calculated as:

$$q_{e1(pH)} = \frac{Q_{1(p_H)}}{n} \tag{32}$$

$$q_{e2(pH)} = \frac{Q_{2(p_H)}}{n} \tag{33}$$

If a flow meter is located in the motor outflow line the component Q_{Le} is omitted. It should be noted that the $q_{e(pH)}$ is a nonlinear function of pressure drop Δp_i in the working mechanism and is directly proportional to the inverse of the motor shaft speed n.

4.3. Theoretical working volume

If the pressure drop Δp_i in the motor decreases then the leakages Q_L in motor decreases also. Therefore, the value of $q_{e(pH)}$, described by formulas (25) and (26), tends to certain value q_n:

$$\lim_{\Delta p_i \to 0} \left(q_{e1(pH)}\right)_{(n)} = q_{t1} + \Delta q_L = q_{n1} \tag{34}$$

$$\lim_{\Delta p_i \to 0} \left(q_{e2(pH)}\right)_{(n)} = q_{t2} + \Delta q_L = q_{n2} \tag{35}$$

The share of leakages Q_L in general flow rate in the motor decreases if rotational speed n increases. Thus, the theoretical working volume can be axpressed as:

$$\lim_{n\to\infty}(q_{n1}) = q_{t1} \tag{36}$$

$$\lim_{n\to\infty}(q_{n2}) = q_{t2} \tag{37}$$

The graphical interpretation of q_n and theoretical working volume q_t is shown in Fig. 3.

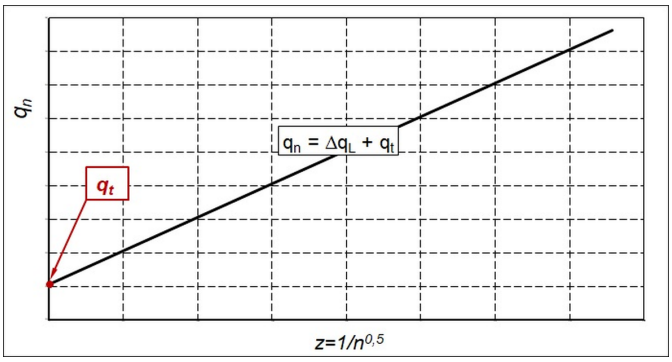

Fig. 3. The graphical implementation of the new method.

As a final theoretical working volume is proposed:

$$q_t = 0.5\cdot(q_{t1} + q_{t2}) \tag{38}$$

In general, it is advisable to use flow meters of the same type and class to measure flow rates Q_1 and Q_2. Furthermoref the compressibility of liquid is considered, then:

$$q_{t1} = q_{t2} = q_t \tag{39}$$

In practice, only one flowmeter is used in the test stand measuring system. In such a case $q_t = q_{t1}$ or $q_t = q_{t2}$.

4.4. Assesment of the determined value of actual and theoretical working volume

The correctness of the determination of the value of the actual and theoretical workin volume can be assessed using the definitions of mechanical efficiency η_m and volumetric efficiency η_v. For hydraulic motor [36, 37]:

$$\eta_m = 2\cdot\frac{M}{q_r\cdot\Delta p_i} \tag{40}$$

$$\eta_v = \frac{q_r\cdot n}{Q_1} \tag{41}$$

Threrefore for any rotational speed n of the motor and for $\Delta p_i \to 0$ the volumetric efficiency should be $\eta_v < 1$. Furthermore for $\Delta p_i = 0$ is and $q_r = q_t$. If rotational speed of the tested motor is minimum (n_{min}), can be assumed that for $\Delta p_i = 0$ is $\eta_v \approx 1$. Therefore:

$$q_{t(\max)} \le \frac{Q_1}{n_{min}} \tag{42}$$

For assessment of the minimum theoretical working volume $q_{t(min)}$ and actual working volume $q_{r(min)}$ the maximum mechanical efficiency η_m of hydraulic motor should be observed in all range of operating parameters (that is speed n and load M). If $\eta_m \le 1$, then:

$$q_{t(\min)} < q_{r(\min)} \le 2\pi\cdot\frac{M}{\Delta p_i} \tag{43}$$

To sum up:

$$\frac{Q_1}{n_{min}} \ge q_t < 2\pi\frac{M}{\Delta p_i} \tag{44}$$

4.5. General test procedure

In order to obtain experimental data and determine the q_t and q_r the flow Q_1 or Q_2 (at T_1 = cosnt) should be measured firstly for several values of n and for several constant values of Δp. Then should be calculate the Δp_{ich} according to the method described in [35, 38]. After determining the Δp_{ich}, it is possible to calculate the Δp_i. If the flow meter is located in the low-pressure line the $Q_{(pH)}$ should be calculated. Next, the characteristics $q_e = f(\Delta pi)_{n=const}$ should be developed and calculate the q_{r1} (or q_{r2}). Finally, the characteristics $q_r = f(n)$ should be plotted and the walue of q_{t1} (or q_{t2}) should be calculated.

5. Results of experiment

5.1. Object of research

The object of research was a prototype of a satellite hydraulic motor (Fig. 4 and Fig. 5). The principle of operation of the satellite engine is widely known and is described, inter alia, in [23, 34, 36, 37, 39, 41, 54].

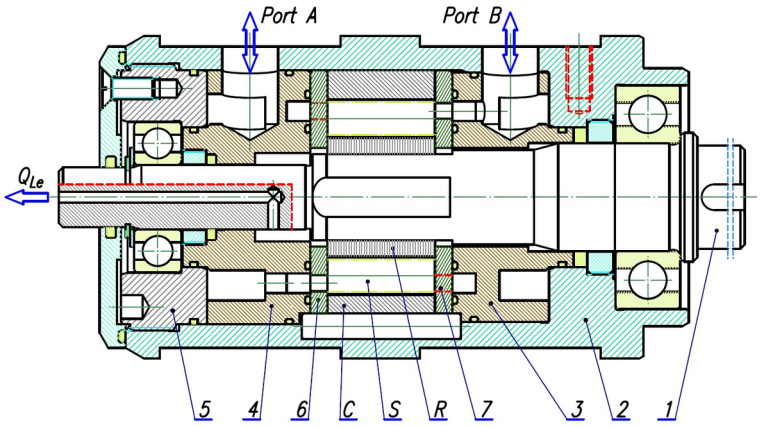

Fig. 4. Tested motor (satellite motor) [36, 37, 39]: C – curvature, S – satellite, R – rotor, 1 – shaft, 2 – case, 3 – inflow/outflow manifold, 4 – outflow/inflow manifold, 5 – rear body, 6 and 7 – distribution (compensation) plates

The geometrical working volume q_g of the tested motor is 34.44 cm^3/rev. This working volume depends on the height H of the working mechanism, areas of the minimum and maximum working chamber (A_{min} and A_{max} – Fig. 5) and the numbers of the humps of the rotor and the curvature (n_R and n_C respectively). The geometrical working volume q_g was calculated according to [36, 37, 39]:

$$q_g = n_C\cdot n_R\cdot H\cdot(A_{max} - A_{min}) \tag{45}$$

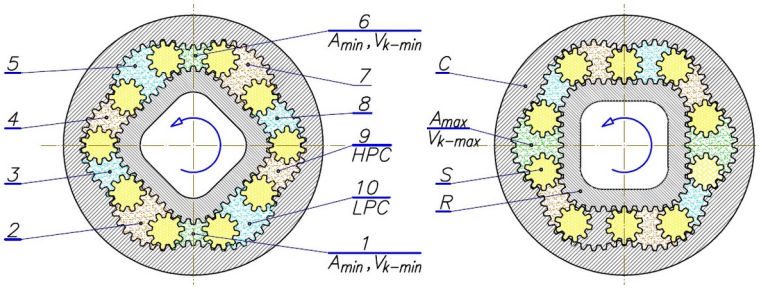

Fig. 5. Working (satellite) mechanism [23, 34, 36, 37, 41, 54]: C – curvature, R – rotor, S – satellite, 1÷10 – working chambers, HPC – high pressure chambers, LPC – low pressure chambers, $V_{k\text{-}min}$ – dead chamber, $V_{k\text{-}max}$ – working chamber with maximum volume and with maximum area A_{max}

where $n_C = 6$, $n_R = 4$, H = 25 mm, $A_{min} = 26.11$ mm^2 and $A_{max} = 83.51$ mm^2.

5.2. The measuring system

The diagram of hydraulic and the measuring system of the test stand is shown in Fig. 6.

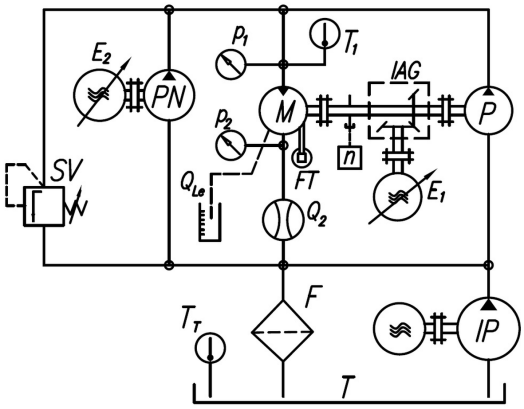

Fig. 6. The test stand measuring system [36, 37, 41]: P – pump, M – tested motor, PN – pump for filling leaks in P and M, IP – impeller pump, SV – safety valve, F – filter, T – tank, IAG – intersecting axis gear, E_1 and E_2 – electric motors with frequency converters, T_1, T_T – temperature sensors, Q_2 – flowmeter, Q_{Le} – leakage measurement, FT – force transducer for torque measurement, n – inductive sensor for measure of rotational speed.

The following measuring instruments were installed in the measuring system of the test stand (Fig. 6):

- two strain gauge pressure transducers (p_1 and p_2) with ranges of 2.5,10,40 MPa and class 0.3;
- piston flowmeter (Q_2) with volume of measured chamber 0.63dm^3, a range of 200 l/min and class 0.2;
- strain gauge force transducer FT for measurement of the torque M with a range of 100 N and class 0.1;
- inductive sensor for measurement of the rotational speed n of the motor shaft with accuracy of ±0.01 rpm);
- RTD temperature sensor with class A and max. measurement error 0.5 °C – for measurement of the liquid temperature T_1 in the inflow port of the motor.

Pressure drop Δp, speed n and oil temperature T_1 settings were made very precisely, with as few deviations as possible. Thus, for speed ±0.1 rpm, for pressure drop ±0.05 MPa and for temperature ±1.0 °C. Each recorded measurement result is the average of three repetitions. This regime of parameter settings enabled to determine the working volume with the lowest possible error.

A valuable advantage of the piston flow meter should also be highlighted here. Well, it measured the average flow rate from more than 18 revolutions of the motor shaft (due to the large volume of the flow meter's measuring chamber of as much as 0. 63dm^3)!

5.3. Working liquid parameters

The working liquid in test stand was the Total Azolla ZS 46 oil. The research was conducted with the temperature in the motor inflow port T_1 = 43 °C (ν = 40 cSt, ρ = 873 kg/m^3). According to the proposed new method, the characteristic of tangential isentropic bulk modulus $K_{Z(p)}$ of mineral oil is needed to correct determine the theoretical and actual working volume. This characteristic was shown in Fig. 7 [55].

5.4. Characteristics of flow rate in the outflow line of the motor

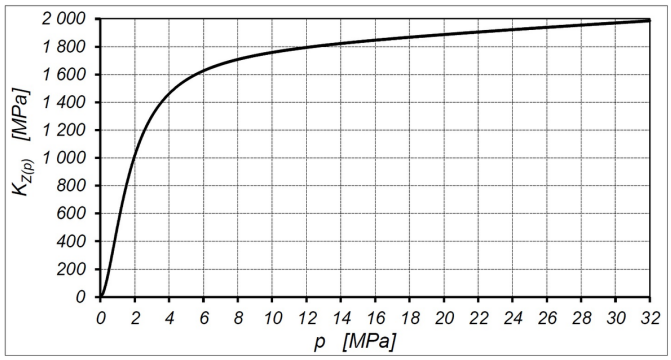

Fig. 7. Bulk modulus $K_{Z(p)}$ of Total Azolla ZS 46 mineral oil [36, 37, 55]

The motor tests were carried out for in the pressure drop range Δp up to 32 MPa and in the range of rotational speed n from 50 to 1500 rpm. The flow rate Q_2 was measured over the entire pressure drop Δp range at n = const. (Fig. 8).

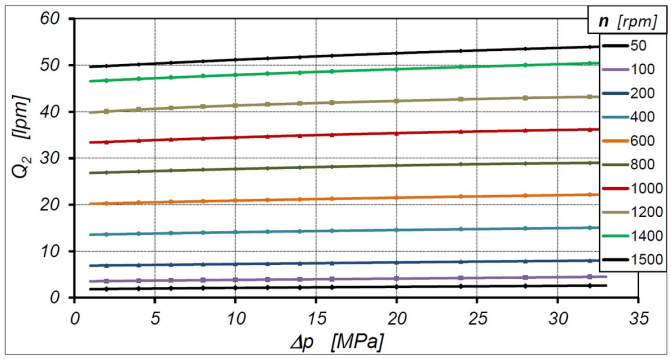

Fig. 8. Flow rate Q_2 vs Δp at n = const

The external leakage Q_{Le} in the tested motor was exceedingly small regardless of rotational speed n (Fig. 9).

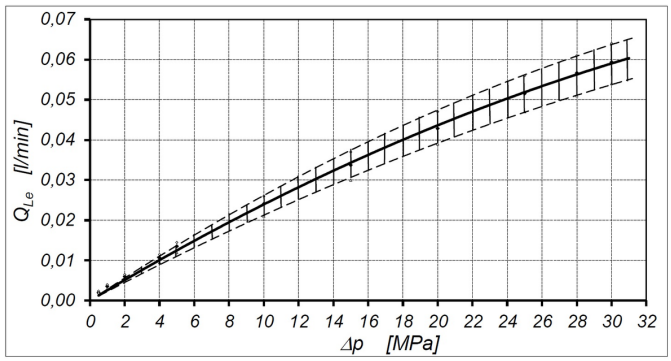

Fig. 9. External leakage Q_{Le} in tested motor [36]

5.5. Characteristics of flow rate vs pressure drop in working mechanism

Pressure drop Δp_{ich} in internal channels of the tested motor was calculated according to the formula (6):

$$\Delta p_{ich} = 0.003224 \cdot Q_2^2 + 0.02183 \cdot Q_2 \tag{46}$$

where Q_2 in [l/min] and Δp_{ich} in [MPa] [35, 36, 38].

In Fig. 10 characteristics $Q_2 = f(\Delta p_i)$ at n = const. are shown. The pressure drop Δp_i in working mechanism was calculated according to formula (5) and (46). The influence of liquid compressibility was omitted.

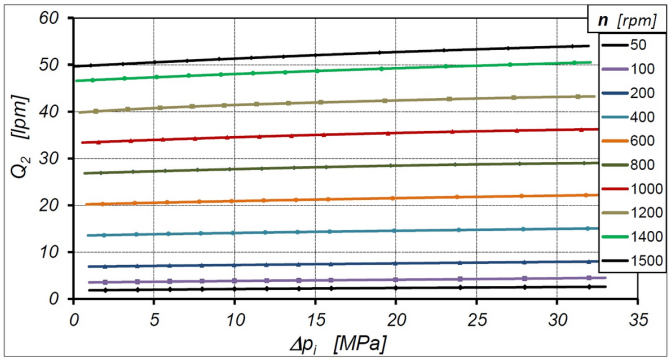

Fig. 10. Flow rate Q_2 vs Δp_i at n = const. The influence of liquid compressibility was omitted

The flow rate $Q_{2(pH)}$ is related to the pressure p_H in the high-pressure chamber of the motor. Values of $Q_{2(pH)}$ was calculated according to formulas (29) and (31). The characteristics of $Q_{2(pH)} = f(\Delta p_i)$ are shown in Fig. 11.

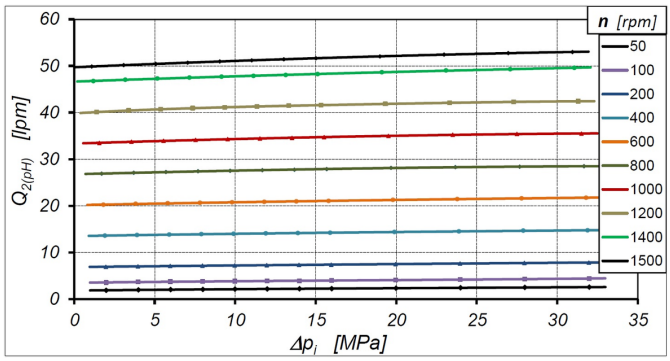

Fig. 11. Flow rate $Q_{2(pH)}$ vs Δp_i at n = const

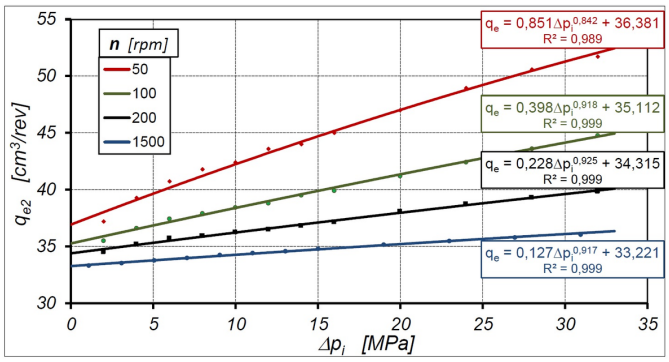

Fig. 12. Characteristics of q_{e2} vs Δp_i at n=const – according to Balawender's method

The characteristics presented in the Fig. 10 and Fig. 11 show that the $Q_{2(pH)}$ is smaller than Q_2. In the whole range of pressure drop Δp_i, the difference does not exceed 2%.

5.6. Theoretical working volume according to Balawender method

The characteristics of $q_{e2} = f(\Delta p_i)$ determined according to Balawender's method are shown in Fig. 12.

From the above characteristics it can be seen that:

- $q_{t(50)} = 36.81$ cm^3/rev;
- $q_{t(100)} = 35.112$ cm^3/rev;
- $q_{t(200)} = 34.315$ cm^3/rev;
- $q_{t(1500)} = 33.221$ cm^3/rev.

Then, according to formula (18) the theoretical working wolume of the satellite motor is $q_t = 34.757$ cm^3/rev.

5.7. Theoretical working volume according to proposed new method

According to proposed new method the characteristics of $q_{e2(pH)} = f(\Delta p_i)$ (shown in Fig. 13) were calculated taking into consideration flow rate $Q_{2(pH)}$ related to the pressure in the high-pressure working chamber (Fig. 11). That is, the values of q_e were calculated according to formula (33). All characteristics of $q_{e2(pH)} = f(\Delta p_i$ have been described by equations. These equations are presented in the Table 1. The characteristics of $q_n = f(1/n^{0.5})$ are shown inFig. 14.

The results of research shown that, according to the new method, the working wolume q_{rn} should be described by equation (35) and then (Fig. 14 – the black line):

$$q_n = 24.989 \cdot n^{-0.5} + 32.527 \tag{47}$$

Table 1. Equations $q_{e(pH)} = f(\Delta p_i^3)$ of motor output flow rate at n = const.

No.	n [rpm]	$q_{e2(pH)} = f(\Delta_{pi}{}^3)$	q_n [cm^3/rev.]	R^2
1	50	$q_{e2(pH)} = 0.000207\Delta p_i^3 - 0.014881\Delta p_i^2 + 0.725139\Delta p_i + 36.1738$	36.1738	0.9944
2	100	$q_{e2(pH)} = 0.000149\Delta p_i^3 - 0.007912\Delta p_i^2 + 0.383909\Delta p_i + 34.8875$	34.8875	0.9969
3	200	$q_{e2(pH)} = 0.000007\Delta p_i^3 - 0.001087\Delta p_i^2 + 0.179735\Delta p_i + 34.2685$	34.2685	0.9962
4	400	$q_{e2(pH)} = 0.000023\Delta p_i^3 - 0.002158\Delta p_i^2 + 0.144543\Delta p_i + 33.7095$	33.7095	0.9979
5	600	$q_{e2(pH)} = 0.000006\Delta p_i^3 - 0.001128\Delta p_i^2 + 0.114055\Delta p_i^2 + 33.5305$	33.5305	0.9985
6	800	$q_{e2(pH)} = -0.000009\Delta p_i^3 - 0.000939\Delta p_i^2 + 0.107023\Delta p_i + 33.4235$	33.4235	0.9979
7	1000	$q_{e2(pH)} = -0.000000\Delta p_i^3 - 0.001292\Delta p_i^2 + 0.110816\Delta p_i + 33.2959$	33.2959	0.9983
8	1100	$q_{e2(pH)} = 0.000032\Delta p_i^3 - 0.002719\Delta p_i^2 + 0.122427\Delta p_i + 33.2802$	33.2802	0.9983
9	1200	$q_{e2(pH)} = 0.000044\Delta p_i^3 - 0.003723\Delta p_i^2 + 0.142850\Delta p_i + 33.2614$	33.2614	0.9991
10	1300	$q_{e2(pH)} = 0.000017\Delta p_i^3 - 0.001736\Delta p_i^2 + 0.107760\Delta p_i + 33.2487$	33.2487	0.9986
11	1400	$q_{e2(pH)} = 0.000007\Delta p_i^3 - 0.000913\Delta p_i^2 + 0.090225\Delta p_i + 33.2403$	33.2403	0.9986
12	1500	$q_{e2(pH)} = -0.000001\Delta p_i^3 - 0.000870\Delta p_i^2 + 0.100618\Delta p_i + 33.2245$	33.2245	0.9999

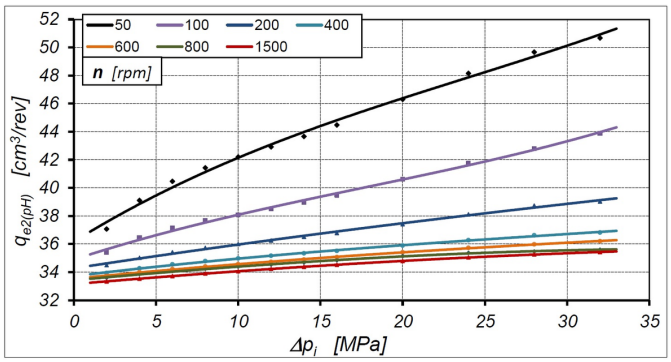

Fig. 13. Characteristics $q_{e2(pH)}$ vs Δp_i at n = const – according to the new method. Equations in Table 1

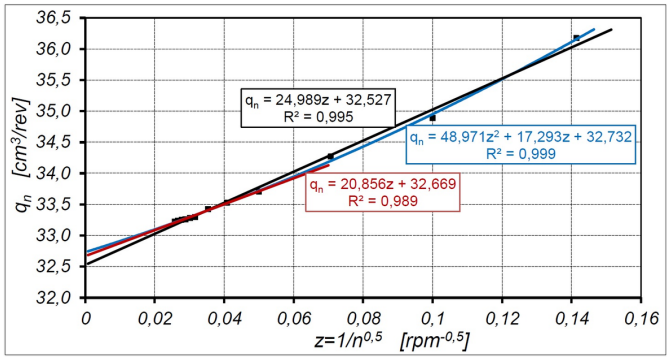

Fig. 14. Characteristics of working volume q_n vs n (according to the new method)

That is, the theoretical working volume of satellite motor is q_t = 32.527 cm^3/rev.

Newertheless, the results of experiment, shown in Fig. 14, indicate some non-linearity between q_n and $n^{-0.5}$ (the blue characteristic in Fig. 14). Then the Δq_L is better to describe by following empirical formula:

$$\Delta q_L = \left(\frac{C_{id1}}{n} + \frac{C_{id2}}{n^{0.5}} \right) \cdot m^2 \cdot H \tag{48}$$

It has been observed that if results for low speed n of motor will be neglected, then the linear relationship between q_n and $n^{-0.5}$ (the red line in Fig. 14) gives similar result in q_t like nonlinear relationship (the blue line in Fig. 14). It is supposed that, the additional flow rate depends on the speed n can exist in commutation unit of the satellite motor. Furthermore, at the present time, it seems reasonable to ignore low rotational speeds in the search of theoretical working volume q_t. For tested motor was ignored the low speed up to 400 rpm (the red line in Fig. 14). Then as the theoretical working volume of satellite motor should be adopted q_t = 32.669 cm^3/rev. The relative difference between the q_t = 32.527 cm^3/rev for all range of motor speed n (the black line in Fig. 14) in about 0.44%.

6. The assessment of actual working volume

Taking into consideration formulas (22) and (33) and the formulas from Table 1 is possible to assess the actual working volume q_r in tested hydraulic motor. Theoretically the q_r would be independent on rotational speed n. But results of experiment show some deviations. In Fig. 15 are shown selected characteristics of Δq_p plotted according to equations from Table 1.

It can be seen that for n > 800 rpm the Δq_p takes a constant value. Characteristics of $\Delta q_p = f(\Delta p_i)$ for n > 800 rpm are shown in Fig. 16.

Therefore, taking into account formula (22), the actual working volume q_r is:

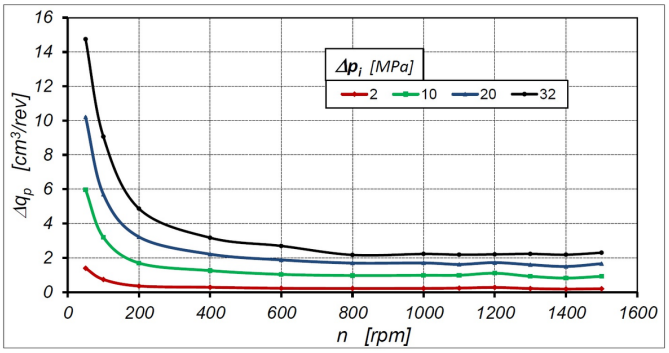

Fig. 15. Characteristics of Δq_p plotted according to equations from Table 1

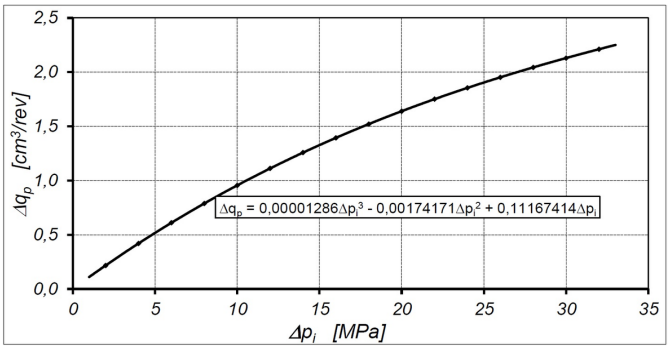

Fig. 16. Characteristics of Δq_p vs Δp_i for n > 800 rpm

$$q_r = 32{,}669 + 0{,}11167414 \cdot \Delta p_i + 0{,}00174171 \cdot \Delta p_i^{\,2} + 0{,}00001286 \cdot \Delta p_i^{\,3} \quad [\text{cm}^3/\text{rev.}] \tag{49}$$

Thus, the results of experiment confirm the theoretical considerations. That is, the pressure drop Δp_i in motor's working chambers has a significant influence on the actual working volume q_r. Therefore, the actual working volume q_r should be taken into account (instead of theoretical working volume q_t) for calculation the volumetric losses and mechanical losses in hydraulic motor (and the same volumetric efficiency and mechanical efficiency).

7. Discussion

The characteristics presented in the Fig. 10 and Fig. 11 show that the $Q_{2(pH)}$ is smaller than Q_2. In the whole range of pressure drop Δp_i. The difference does not exceed 1,6%. This difference is typical of mineral oil [54] and has an effect on the characteristics of flow rate per one revolution of the motor shaft (Fig. 13) and finally on the theoretical working volume q_t.

The analysis of experimental data allow to confirm the theoretical considerations that the q_e is an nonlinear function of Δp for n=const regardless of the used method (Balawender method or the new method).

The value of the correlation coefficient R^2 of nonlinear function $q_e = f(\Delta p)_{n=const}$ is close to one ($R^2 > 0.99$, Table 1). Hence, the conclusion is that equations (25) and (26) very well describe fluid flow per one revolution of the motor shaft.

Based on the results of the motor tests, it can be concluded that regardless of the used method (Balavender or the new method):

a) the rotational speed n has no influence on the theoretical working volume q_t of a hydraulic motor;
b) pressure drop Δp_i in the motor working chambers has no influence on the theoretical working volume q_t of a hydraulic motor;
c) the flow rate q_e per one revolution of the motor shaft is a nonlinear function of pressure drop Δp_i in the motor working chambers (Fig. 12, Fig. 13 and Table 1).

Furthermore the results of the satellite motor test confirm that:

a) is correct to describe the q_e by a third order polynomial (expressed by the formula (25) or (26));
b) the flow rate q_{in} (and the same q_e) is a nonlinear function of the motor rotational speed n. The results of experiment and calculations can be described by equation (34) or (35) with sufficient accuracy ($R^2 = 0.995$ – Fig. 14).

Nonetheless, the theoretical working voume q_t calculated using the new method (q_t = 32.669 cm^3/rev.) is about 6% smaller than q_t calculated using Balawender's method (q_t = 34.757 cm^3/rev.). This difference is not small. Designers of hydraulic positive displacement machines and researchers conducting development studies on these machines should therefore follow the method proposed in this article. Incorrectly adopted the value of the theoretical working volume gives an incorrect assessment of mechanical and volumetric losses.

Based on the analysis of the test results, it can be concluded that the motor working volume increases as a function of the pressure drop Δp_i in the motor. For tested motor this increase is 2,2 cm^3/rev. (Fig. 16). This is 6% of the theoretical working volume. It seems like a lot. But when analyzing the structure of the satellite mechanism in the engine (Fig. 4 and Fig. 5), it is concluded that the stiffness of the curvature and the planet are small. Thus, such an increase in the working volume at a pressure of 32 MPa is real.

Furthermore, characteristics of volumetric efficiency and mechanical efficiency are the test for correctness of the theoretical working volume assessment, because the maximum value of these efficiencies cannot be bigger than 1. If the theoretical working volume, calculated using the Balawender method, is taken, the volumetric efficiency of the motor for Δp < 15 MPa is larger than 1 ($\eta_v > 1$) (Fig. 17). It has no physical sense and the conclusion should be that the theoretical working volume has been miscalculated. Therefore, it confirms, that the Balawender's method is inaccurate and overestimates the theoretical working volume. Furthermore, for q_t = 34,757 cm^3/rev. the mechanical efficiency is understated (Fig. 18).

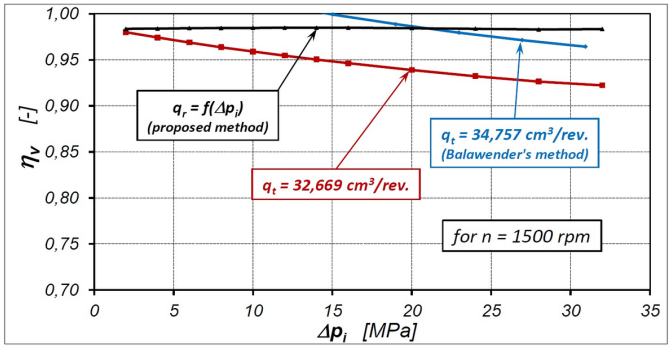

Fig. 17. Volumetric efficiency η_v vs Δp_i of tested motor (n = 1500 rpm) – comparison for q_t according to Balawender method and proposed new method.

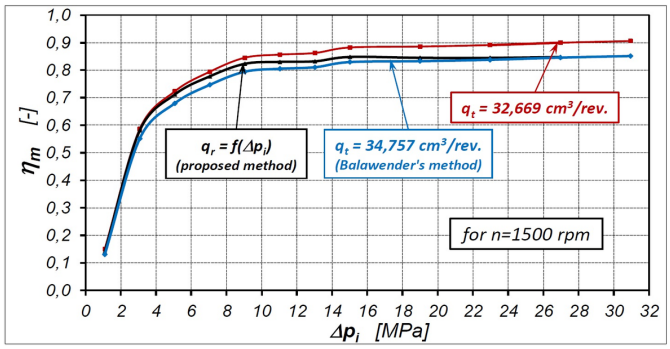

Fig. 18. Mechanical efficiency η_m vs Δp_i of tested motor (n = 1500 rpm) – comparison for q_t according to Balawender method and proposed new method.

On the above figures, characteristics of efficiencies for actual working volume q_r are also shown. Volumetric efficiency is nearly constant in all range of pressure drop Δp_i. It shows that axial clearances of satellites and rotor decreasases under the influence of increasing the pressure drop Δp_i in the motor. Thus, the axial clearance compensation unit in motor operating correctly and the increasing in actual working volume q_r. may be caused by small stiffness of curvature, rotor and teeth in these elements (also in satellites).

The next consideration is the difference between the geometric working volume q_g (34.44 cm^3/rev) and the theoretical working volume q_t (32.669 cm^3/rev) derived from the test results. The relative difference is about 5.5%. Thus, this difference is not small. The geometric working volume q_g results from the CAD drawing documentation. Satellite, curvature and rotor are made by wire electrical discharge machining method (WEDM method). They are made with some technological allowance for finishing treatment (lapping). The size of the allowance and the final geometrical dimensions after lapping are not known – is the secret of the company manufacturing the satellite motors. Furthermore, there are clearances at the tops of the teeth in the satellite mechanism components. In effect is a certain volume included in the geometric working volume. As a result, the geometrical working volume of a satellite motor is smaller than that in the CAD documentation.

8. Conclusions

The new methodology for determining the theoretical and actual working volume of a hydraulic motor is presented in this article.

It has been shown that a simplified approach (consisting in accepting for calculations the flow characteristics as a function of the pressure drop Δp measured in the motor ports and neglecting the liquid compressibility) to the calculation of the theoretical working volume q_t of the hydraulic motor results in an overestimated value of this volume. For the motor presented in this article, the differences are as high as 6%. Thus, an overestimated value of the theoretical working volume results in overestimated volumetric efficiency and understated mechanical efficiency of the motor (calculated according to commonly known definitions, i.e. based on the theoretical working volume) (Fig. 17 and Fig. 18).

The article shows that for a satellite engine, for a theoretical working volume determined in a simplified manner (taking into account Δp), the volumetric efficiency is greater than one in the range of Δp < 15 MPa (Fig. 17). Thus, it proves a considerable inaccuracy of the method known and used so far. To a lesser extent, the overestimated value of the theoretical working volume reduces the value of the mechanical efficiency. This efficiency is underestimated by about 3% (Fig. 18).

Therefore, in order to determine the correct value of the theoretical working volume of a hydraulic motor, an analysis of the flows in the motor as a function of the pressure drop Δp_i in its working chambers should be performed. In order to calculate the Δp_i (according to the formula (5)) it is necessary to determine the pressure drop Δp_{ich} in the internal channels of the motor.

It has also been shown that when determining the theoretical working volume, the compressibility of the liquid should not be neglected. The flow rate $Q_{(pH)}$ corresponding the value of high-pressure p_H in the working chambers should be used for calculations the theoretical working volume.

The test results also confirmed that the working volume increases if the pressure drop Δp_i in this motor increases (Fig. 16 and formula (22)). This working volume was called the actual working volume q_r. It has been shown that the actual working volume q_r should be taken to calculate the volumetric and mechanical losses and also the volumetric and mechanical efficiency of the motor.

In subsequent publications, the influence of the type of liquid on the value of the theoretical and actual working volume of the hydraulic motor will be presented. Similar analyzes will also be carried out for the pump.

References

1. Bak M. Torque capacity of multidisc wet clutch with reference to friction occurrence on its spline connections. Scientific Reports 2021; 11: 21305, https://doi.org/10.1038/s41598-021-00786-6.
2. Balawender A. Analiza energetyczna i metodyka badań silników hydraulicznych wolnoobrotowych (Energy analysis and methodics of testing of low-speed hydraulic motors). Scientific book of the Gdansk University of Technology, Mechanika 1988; 54. Gdansk University of Technology Publishing House.
3. Balawender A. Opracowanie metodyki wyznaczania teoretycznej objętości roboczej pomp i silników hydraulicznych wyporowych (The development of the methodology for the determination of the theoretical working volume of positive displacement pumps and hydraulic motors). PhD dissertation. Gdansk University of Technology: 1974.
4. Banaszek A. Methodology of flow rate assessment of submerged hydraulic ballast pumps on modern product and chemical tankers with use of neural network methods. Procedia Computer Science 2021; 192(4): 1894-1903, https://doi.org/10.1016/j.procs.2021.08.195.
5. Banaszek A, Petrovic R. Problem of non proportional flow of hydraulic pumps working with Constant pressure regulators in big power multipump power pack unit in open system. Technicki Vjesnik 2019; 26(2): 294-301, https://doi.org/10.17559/TV-20161119215558.
6. Ding H. Application of non-circular planetary gear mechanism in the gear pump, Advanced Material Research 2012; 591-593: 2139–2142, https://doi.org/10.4028/www.scientific.net/AMR.591-593.2139.
7. Garcia-Bravo J, Nicholson J. What is the real size of that pump? Fluid Power Journal 2018, https://fluidpowerjournal.com/real-size-pump/.
8. Guo S, Chen J, Lu Y, Wang Y, Dong H. Hydraulic piston pump in civil aircraft: current status, future directions and critical technologies. Chinese Journal of Aeronautic 2020; 33(1): 16-30, https://doi.org/10.1016/j.cja.2019.01.013.
9. Guzowski A, Sobczyk A. Reconstruction of hydrostatic drive and control system dedicated for small mobile platform. Proceedings of the 8th FPNI Ph.D Symposium on Fluid Power. 8th FPNI Ph.D Symposium on Fluid Power. Lappeenranta, Finland. June 11–13, 2014. V001T05A012. ASME, https://doi.org/10.1115/FPNI2014-7862.
10. International Organisation for Standardization. ISO 8426:2008. Hydraulic fluid power – Positive displacement pumps and motors – Determination of derived capacity, https://www.iso.org/standard/40351.html.
11. Jasinski R. Analysis of the heating process of hydraulic motors during start-up in thermal shock conditions. Energies 2022; 15(1): 55, https://doi.org/10.3390/en15010055.
12. Jasinski R. Problems of the starting and operating of hydraulic components and systems in low Ambient Temperature (Part IV): modelling the heating process and determining the serviceability of hydraulic components during the starting-up in low ambient temperature. Polish Maritime Research 2017; 24(3): 45–57, https://doi.org/10.1515/pomr-2017-0089.
13. Karpenko M, Bogdevicius M. Review of energy-saving technologies in modern hydraulic drives. Science – Future of Lithuania 2017; 9(5): 553-558, https://doi.org/10.3846/mla.2017.1074.
14. Karpenko M, Prentkovskis O, Sukevicius S. Research on high-pressure hose with repairing fitting and influence on energy parameter of the hydraulic drive. Eksploatacja i Niezawodnosc – Maintenance and Reliability 2022; 24(1): 25–32, http://doi.org/10.17531/ein.2022.1.4.
15. Kim T, Kalbfleisch P, Ivantysynova M. The effect of cross porting on derived displacement volume. International Journal of Fluid Power 2014; 15(2): 77-85, https://doi.org/10.1080/14399776.2014.923605.
16. Klarecki K, Rabsztyn D, Hetmanczyk P. Analysis of pulsation of the sliding-vane pump for selected settings of hydrostatic system. Eksploatacja i Niezawodnosc – Maintenance and Reliability 2015; 17(3): 338–344, http://dx.doi.org/10.17531/ein.2015.3.3.
17. Kollek W, Osinski P, Stosiak M, Wilczynski A, Cichon P. Problems relating to high-pressure gear micropump. Archives of Civil and Mechanical Engineering 2014; 14(1): 88-95, https://doi.org/10.1016/j.acme.2013.03.005.
18. Li D, Liu Y, Gong J, Wang T. Design of a noncircular planetary gear mechanism for hydraulic motor. Mathematical Problems in Engineering 2021; https://doi.org/10.1155/2021/5510521.
19. Lisowski E, Filo G, Rajda J. Analysis of the energy efficiency improvement in a load-sensing hydraulic system built on the ISO plate. Energies 2021; 14(20): 6735, https://doi.org/10.3390/en14206735.
20. Luan Z, Ding M. Research on non-circular planetary gear pump. Advanced Material Research 2021; 339: 140-143, https://doi.org/10.4028/www.scientific.net/AMR.339.140.
21. Manring N, Williamson C. The theoretical volumetric displacement of a check-valve type, digital displacement pump. Journal of Dynamic System, Measurement and Control 2019; 141(3), https://doi.org/10.1115/1.4041713.
22. Michael P, Garcia-Bravo J. The determination of hydraulic motor displacement. Proceedings of the 17th Scandinavian International Conference on Fluid Power SICFP'21. Linkoping, Sweden. June 1-2, 2021, https://doi.org/10.3384/ecp182p188.
23. Oshima S, Hirano T, Miyakawa S, Ohbayashi Y. Development of a rotary type water hydraulic pressure intensifier. JFPS International Journal of Fluid Power System 2009; 2(2): 21-26, https://doi.org/10.5739/jfpsij.2.21.
24. Oshima S, Hirano T, Miyakawa S, Ohbayashi, Y. Study on the output torque of a water hydraulic planetary gear motor. Proceedings of the the Twelfth Scandinawian International Conference on Fluid Power. Tampere, Finland. May 18-20, 2011.
25. Osiecki L. Mechanizmy rozrządu hydraulicznych maszyn wielotłoczkowych osiowych (Commutation units of hydraulics axial piston machines). Monografie 2006; 72. Gdansk University of Technology Publishing House.
26. Osinski P, Deptula A, Partyka M. Hydraulic tests of the PZ0 gear micropump and the importance rank of its design and operating parameters. Energies 2022; 15(9): 3068, https://doi.org/10.3390/en15093068.
27. Osinski P, Warzynska U, Kollek W. The influence of gear micropump body asymmetry on stress distribution. Polish Maritime Research 2017; 24(1): 60-65, https://doi.org/10.1515/pomr-2017-0007.
28. Patrosz P. Influence of gaps' geometry change on leakage flow in axial piston pumps. In: Stryczek J., Warzyńska U. (eds) Advances in Hydraulic and Pneumatic Drives and Control 2020. NSHP 2020. Lecture Notes in Mechanical Engineering. Springer, Cham., https://doi.org/10.1007/978-3-030-59509-8_7.
29. Pobedza J, Sobczyk A. Properties of high-pressure water hydraulic components with modern coatings. Advanced Materials Research 2014; 849: 100-107, https://doi.org/10.4028/www.scientific.net/AMR.849.100.
30. Post W. Models for steady-state performance of hydraulic pumps: determination of displacement. Proceedings of the 9th Bath International Fluid Power Workshop. University of Bath, United Kingdom. September 9-11, 1996; 9: 339-352, https://research.tue.nl/en/publications/models-for-steady-state-performance-of-hydraulic-pumps-determinat.

31. Saheban Alahadi M J, Shirneshan A, Kolahdoozan M. Experimental investigation of the effect of grooves cut over the piston surface on the volumetric efficiency of a radial hydraulic piston pump. International Journal of Fluid Power 2017; 18(3): 181-187, https://doi.org/10.1080/14399776.2017.1337440.
32. Schlosser W M J, Hilbrands J W. Das theoretische Hubvolumen von Verdrangerpumpen. Olhydrauli und Pneumatik 1963; 4.
33. Schlosser W M J, Hilbrands J W. Das volumetrische Wirkungsgrad von Verdrongerpumpen. Olhydrauli und Pneumatik 1963; 12.
34. Sliwinski P, Patrosz P. Patent PL218888 Satelitowy mechanizm roboczy hydraulicznej maszyny wyporowej (Satellite operating mechanism of the hydraulic displacement machine). 2015; https://ewyszukiwarka.pue.uprp.gov.pl/search/pwp-details/P.401821.
35. Sliwinski P, Patrosz P. The influence of water and mineral oil on pressure losses in hydraulic motor. In: Stryczek J., Warzyńska U. (eds) Advances in Hydraulic and Pneumatic Drives and Control 2020. NSHP 2020. Lecture Notes in Mechanical Engineering. Springer, Cham. https://doi.org/10.1007/978-3-030-59509-8_10.
36. Sliwinski P. Determination of the theoretical and actual working volume of a hydraulic motor. Energies 2020; 13(22): 5933, https://doi.org/10.3390/en13225933.
37. Sliwinski P. Determination of the theoretical and actual working volume of a hydraulic motor – Part II (The method based on the characteristics of effective absorbency of the motor). Energies 2021; 14(6): 1648, https://doi.org/10.3390/en14061648.
38. Sliwinski P, Patrosz P. Methods of determining pressure drop in internal channels of a hydraulic motor. Energies 2021; 14(18): 5669. https://doi.org/10.3390/en14185669.
39. Sliwinski P. Satelitowe maszyny wyporowe. Podstawy projektowania i analiza strat energetycznych. (Satellite displacement machines. Basic of design and analysis of power loss). Monografie 2016; 155. Gdansk University of Technology Publishing House.
40. Sliwinski P. The influence of water and mineral oil on volumetric losses in hydraulic motor. Polish Maritime Research 2017; 24 (s1): 213–223, https://doi.org/10.1515/pomr-2017-0041.
41. Sliwinski P. The influence of water and mineral oil on mechanical losses in a hydraulic motor for offshore and marine application. Polish Maritime Research 2020; 27(2): 125-135, https://doi.org/10.2478/pomr-2020-0034.
42. Stawinski L, Kosucki A, Cebulak M, Gorniak vel Gorski A, Grala M. Investigation of the influence of hydraulic oil temperature on the variable-speed pump performance. Eksploatacja i Niezawodnosc – Maintenance and Reliability 2022; 24(2): 289–296, http://doi.org/10.17531/ein.2022.2.10.
43. Stryczek S. Napęd hydrostatyczny (Hydrostatic drive). PWN: 2016.
44. Toet G, Johnson J, Montague J, Torres K, Garcia-Bravo J. The determination of the theoretical stroke volume of hydrostatic positive displacement pumps and motors from volumetric measurements. Energies 2019; 12(3): 415, https://doi.org/10.3390/en12030415.
45. Toet G. Die Bestimmung des theoretischen Hubvolumens von hydrostatischen Verdrangerpumen und Motoren aus volumetrischen Messungen. Olhydraulik Pnaumatik 1970; 14.
46. Ulanowicz L, Jastrzebski G, Szczepaniak P. Method for estimating the durability of aviation hydraulic drives. Eksploatacja i Niezawodnosc – Maintenance and Reliability 2020; 22(3): 557–564, http://dx.doi.org/10.17531/ein.2020.3.19.
47. Volkov G, Fadyushin D V. Improvement of the method of geometric design of gear segments of a planetary rotary hydraulic machine. Journal of Physics: Conference Series 2021; 1889: 042052, https://iopscience.iop.org/article/10.1088/1742-6596/1889/4/042052.
48. Volkov G, Smirnov V, Mirchuk M. Estimation and ways of mechanical efficiency upgrading of planetary rotary hydraulic machines. IOP Conference Series: Materials Science and Engineering 2020; 709: 022055, https://iopscience.iop.org/article/10.1088/1757-899X/709/2/022055.
49. Volkov G, Smirnov V. Systematization and comparative scheme analysis of mechanisms of planetary rotary hydraulic machines. International Conference on Modern Trends in Manufacturing Technologies and Equipment ICMTMTE 2018; 224: 02083, https://doi.org/10.1051/matecconf/201822402083.
50. Wang C, Luan Z, Gao W. Design of pitch curve of internal-curved planet gear pump strain in type N-G-W based on three order ellipse. Advanced Material Research 2013; 787: 567-571, https://doi.org/10.4028/www.scientific.net/AMR.787.567.
51. Wilson W E. Performance criteria for positive displacement pumps and fluid motors. Transition ASME 1949; 71(2).
52. Wu X, Chen C, Hong C, He Y. Flow ripple analysis and structural parametric design of a piston pump. Journal of Mechanical Science and Technology 2017; 31, 4245–4254, https://doi.org/10.1007/s12206-017-0823-8.
53. Zaluski P. Experimental research of an axial piston pump with displaced swash plate axis of rotation. In: Stryczek J., Warzyńska U. (eds) Advances in Hydraulic and Pneumatic Drives and Control 2020. NSHP 2020. Lecture Notes in Mechanical Engineering. Springer, Cham., https://doi.org/10.1007/978-3-030-59509-8_12.
54. Zaluski P. Influence of fluid compressibility and movements of the swash plate axis of rotation on the volumetric efficiency of axial piston pumps. Energies 2022; 15(1): 298. https://doi.org/10.3390/en15010298.
55. Zaluski P. Wpływ położenia osi obrotu tarczy wychylnej na sprawność objętościową pomp wielotłoczkowych osiowych (Influence of the position of the swash plate rotation axis on the volumetric efficiency of axial piston pumps). Ph.D. dissertation. Gdansk University of Technology: 2017.
56. Zhang B, Song S, Jing C, Xiang D. Displacement prediction and optimization of a non-circular planetary gear hydraulic motor, Advances in Mechanical Engineering 2021; 13(11): 1–13, https://doi.org/10.1177/16878140211062690.
57. Zhao H, Wang B, Chen G. Numerical study on a rotational hydraulic damper with variable damping coefficient. Scientific Reports 2021; 11: 22515, https://doi.org/10.1038/s41598-021-01859-2.